CrossMark

TECHNICAL ARTICLE

Powder diffraction study of Pd_2HgSe_3

F. Laufek,[a] A. Vymazalová, and M. Drábek
Czech Geological Survey, Geologická 6, 152 00 Praha 5, Czech Republic

(Received 8 March 2017; accepted 6 September 2017)

The Pd_2HgSe_3 phase was synthetized from individual elements by the silica glass tube technique and its crystal structure has been refined by the Rietveld method. The Pd_2HgSe_3 phase crystalizes in $P\bar{3}m1$ space group with the unit-cell parameters $a = 7.3096(2)$ Å, $c = 5.2829(1)$ Å, $V = 244.45(1)$ Å^3, $D_c = 8.84$ g/cm^3, and $Z = 2$. In its layered crystal structure, the [$PdSe_6$] octahedra share opposing Se–Se edges with adjacent [$PdSe_4$] squares forming layers parallel with the (001) plane. The layers show AA type stacking along the *c*-axis. Hg atoms occupy the anti-cubooctahedral voids between two consecutive layers. Pd_2HgSe_3 is isostructural with Pt_2HgSe_3 and $Pt_4Tl_2X_6$ (X = S, Se, or Te) phases. The structure can be viewed as a $2a.2a.c$ superstructure of $PtSe_2$. © *2017 International Centre for Diffraction Data*. [doi:10.1017/S0885715617001026]

Key words: Pd_2HgSe_3, crystal structure, Rietveld refinement, Pd–Hg–Se system, X-ray powder diffraction data

I. INTRODUCTION

Paar *et al*. (1998) reported a discovery of a Pd_2HgSe_3 phase in the form of a small inclusion of approximately 20 μm in size from carbonate veins in Hope's Nose, Torquay, Devon, England. This phase was first synthetized by Drábek *et al*. (2014) in his systematic investigation of phase relations in the Hg–Pd–Se system. Drábek *et al*. (2014) described the trigonal symmetry of the Pd_2HgSe_3 compound and indicated its unit-cell parameters. However, its crystal structure has been hitherto unknown. Besides the phase Pd_2HgSe_3, two other ternary phases were reported in the Hg–Pd–Se system: mineral tischendorfite $Pd_8Hg_3Se_9$ (Stanley *et al*., 2002) and a synthetic phase Pd_5HgSe (Laufek *et al*., 2012). A Pt-bearing analogue, a phase Pt_2HgSe_3, was described as a mineral jacutingaite by Vymazalová *et al*. (2012).

In this contribution, we present a Rietveld crystal structure analysis of the phase Pd_2HgSe_3. Powder diffraction data up to 130° 2θ (Co$K\alpha$) are also reported. Part of this work was presented in a conference abstract (Laufek *et al*., 2011).

II. EXPERIMENTAL

The ternary Pd_2HgSe_3 phase was prepared using silica glass tube technique. Stoichiometric amounts of palladium (Aldrich 99.99%), mercury (Lachema, 99.999%), and selenium (Aldrich, 99.999%) were used as starting materials for synthesis. The following amounts of reagents were used for synthesis: 0.0658 g of palladium (0.6180 mmol), 0.0620 g of mercury (0.3090 mmol), and 0.0732 g of selenium (0.9270 mmol). The evacuated tube with the carefully weighted charge was at first heated at 800 °C for 24 h. After cooling in a cold-water bath, the charge was removed from the tube and gently ground to powder in acetone using a pestle and an agate mortar. Afterwards, the pulverized charge was again sealed in an evacuated silica glass tube and heated at 400 °C for 41 days. After heating, the sample was quenched in a cold-water bath.

Chemical analyses (EMPA) of Pd_2HgSe_3 phase were performed with a Cameca SX-100 electron microprobe using the wavelength-dispersion mode. Accelerating voltage was set to 15 kV, and the beam current was 10 nA. X-ray lines and standards were as follows: Se$L\alpha$ (pure Se), Pd$L\alpha$ (pure Pd), and Hg$M\alpha$ (HgS). Data were acquired (11 analyses) from different spots on several grains and then averaged. The chemical data yielded an overall composition Pd 32.53 wt.%, Hg 30.19 wt.%, Se 36.52 wt.%, and total 99.24 wt.% with empirical formula $Pd_{2.00}Hg_{0.98}Se_{3.02}$ calculated on six atoms per formula unit.

Ideally, the experimental product should consist only of title phase Pd_2HgSe_3. The subsequent phase and Rietveld analysis of diffraction data revealed small admixture of $Pd_8Hg_3Se_9$ (~12 wt.%) and HgSe (~2 wt.%) in the experimental product. These admixtures have very likely occurred because of possible presence of small amounts of selenium and mercury in a vapour phase during the initial stages of solid-state reactions.

III. STRUCTURE REFINEMENT

The powder X-ray diffraction pattern of the sample was collected in the Bragg–Brentano geometry on an X'Pert Pro PANalytical diffractometer, equipped with an X'Celerator detector using Co$K\alpha$ radiation. An iron filter, placed in a diffracted beam, was used to produce pseudo-monochromatic radiation. To minimize background, a flat low-background silicon wafer was used as the specimen holder. The data were collected in the range from 6 to 130° 2θ. A full-width at half maximum of 0.106° 2θ was obtained at 19.497° 2θ indicating well-crystalized sample of Pd_2HgSe_3. The experimental details are summarized in Table I. With the exception of a few peaks attributable to $Pd_8Hg_3Se_9$ (~12 wt.%) and HgSe (~2 wt.%), the diffraction pattern of Pd_2HgSe_3 was indexed

[a]Author to whom correspondence should be addressed. Electronic mail: frantisek.laufek@geology.cz

https://doi.org/10.1017/S0885715617001026 Published online by Cambridge University Press

TABLE I. Experimental conditions.

Instrument	PANalytical X´Pert Pro
Radiation	Co$K\alpha_1$, Co$K\alpha_2$
Detector	X'Celerator
Soller slits	0.02 rad
Divergence slit	0.25°
Anti-scatter slit	0.5°
Step width	0.0167°
Time per step	200 s
Specimen form	Powder
Specimen holder	"Zero" background

using the DICVOL06 programme (Louër and Boultif, 2007) on the basis of a trigonal cell listed in Table II. The unit cell suggested by Drábek *et al*. (2014) was confirmed. The crystal structure of Pd_2HgSe_3 was subsequently refined by the Rietveld method for powder X-ray diffraction data using the FullProf programme (Rodriguez-Carvajal, 1990). The starting structural model for Pd_2HgSe_3 was derived from the structural data of Pt_2HgSe_3 phase, which is known as a mineral jacutingaite (Vymazalová *et al*., 2012). This mineral phase has very similar unit-cell parameters [$a = 7.3477(2)$, $c = 5.2955(1)$ Å] and analogous stoichiometry. Only the Pt atoms were replaced by Pd atoms and the structure was subsequently refined. The structure data for $Pd_8Hg_3Se_9$ and HgSe were taken from the papers of Laufek *et al*. (2014) and Earley (1950), respectively. During the Rietveld refinement, the scale factors and unit-cell parameters of these two phases were refined, while their fractional coordinates and displacement parameters were fixed.

The pseudo-Voigt function was used to generate the shape of the diffraction peaks in the subsequent Rietveld refinement. The background was modelled by the linear interpolation between consecutive breakpoints in the pattern. The refined parameters of Pd_2HgSe_3 include those describing the peak shape and width, peak asymmetry, unit-cell parameters, fractional coordinates, March–Dollase model of preferred orientation along [001] and isotropic displacement parameters for all atoms. Peak asymmetry was modelled using the correction of Bérar and Baldinozzi (1993); two parameters were refined. In total, 24 parameters were refined; 138 reflections were observed. The refinement of preferred orientation correction significantly improved the Rietveld fit; the R_{wp} factor decreased from 4.78 to 2.21%. The G_1 parameter of the March–Dollase correction model was refined to 0.761(1). The final cycles of refinement converged to the residual factors: $R_B = 4.37\%$, $R_{wp} = 2.21\%$, and $R_p = 1.53\%$. The refined atomic coordinates are given in Table II. Figure 1 shows the final Rietveld plot.

TABLE II. Refined parameters for Pd_2HgSe_3 [room temperature, space group $P\bar{3}m1$. $a = 7.3096(2)$ Å, $c = 5.2829(1)$ Å, $V = 244.45(1)$ Å^3, $D_c = 8.84$ g/cm^3, $Z = 2$, $R_p = 1.53\%$, $R_{wp} = 2.21\%$, and $R_B = 4.37\%$, $F(000) = 502$, $\mu = 206.3$ mm^{-1}].

Atom	Site	x	y	z	U_{iso}
Pd(1)	1*a*	0	0	0	0.0064(9)
Pd(2)	3*e*	½	0	0	0.0219(6)
Hg	2*d*	⅓	⅔	0.3591(4)	0.0235(4)
Se	6*i*	0.8303(2)	0.1697(2)	0.2517(3)	0.0217(5)

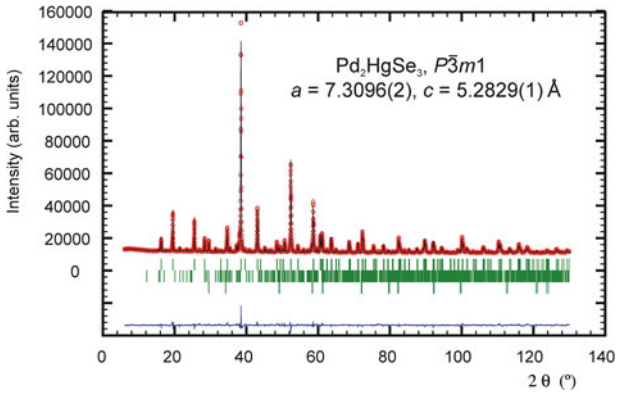

Figure 1. (Color online) The observed (circles), calculated (solid line), and difference Rietveld profiles for Pd_2HgSe_3. The upper reflections bars correspond to Pd_2HgSe_3; the middle and lower bars to 12 and 2 wt.% of $Pd_8Hg_3Se_9$ and HgSe impurities, respectively.

IV. RESULTS AND DISCUSSION

The powder diffraction data are listed in Table III. The observed values of diffraction positions, *d*-spacing, and intensities were extracted by the Topas programme (Bruker AXS, 2014) using the split Pearson VII profile function. The $2\theta_{obs}$ and d_{obs} were corrected for the refined sample displacement correction. No significant diffraction overlap between diffraction patterns of Pd_2HgSe_3 and HgSe occurs. The phase $Pd_8Hg_3Se_9$ (*Pmmn*, $V = 782.5$ Å) shows relatively complex diffraction pattern. Consequently, roughly above 60° of 2θ, there is a noticeable diffraction overlap between patterns of Pd_2HgSe_3 and $Pd_8Hg_3Se_9$. However, considering the low content of $Pd_8Hg_3Se_9$ in a sample and its complex diffraction pattern, its intensity contribution to the diffraction pattern of Pd_2HgSe_3 above 60° of 2θ is negligible.

The crystal structure of Pd_2HgSe_3 is isostructural with mineral jacutingaite, Pt_2HgSe_3 (Vymazalová *et al*., 2012), and synthetic phases $Pt_4Tl_2S_6$, $Pt_4Tl_2Se_6$, $Pt_4Tl_2Te_6$, and $Pd_4Tl_2Se_6$ (Bronger and Bonsmann, 1995). The structure contains two independent Pd positions, one Hg and one Se position. The Pd(1) atom is surrounded by six Se atoms at 2.526 (2) Å forming a slightly distorted octahedron with intra-octahedral Se–Pd(1)–Se angles 85.14(5)° and 94.85(5)° instead of 90° being for a regular octahedron. Unlike the Pd(1) atom, the Pd(2) atom forms a square planar configuration with four Se atoms at a distance of 2.478(2) Å. The coordination of the Pd(2) atom is further completed by two Hg atoms at 2.837(1) Å. The vector of Pd–Hg bonds is almost perpendicular to the [$PdSe_4$] squares. This Pd–Hg distance is comparable to 2.82 Å found in PdHg (Terada and Cagle, 1960) indicating significant Pd–Hg bonding interactions.

As is shown in Figure 2, the [$PdSe_6$] octahedra shares six Se–Se edges with adjacent [$PdSe_4$] squares forming layers parallel to the (001) plane. The layers are stacked along the *c*-axis and show the AA type of stacking. It is interesting to note that the [$PdSe_6$] octahedra have a shared edge length [$d_{Se-Se} = 3.419(2)$ Å] considerably shorter than its unshared edge [$d_{Se-Se} = 3.721(2)$ Å], which is in agreement with the Pauling third rule (Pauling, 1929). The [$PdSe_4$] squares also show two different Se–Se edge lengths: 3.419(2) and 3.588(2) Å for the shared and unshared edges, respectively. This brings the Pd–Pd separation to 3.655(1) Å and consequently reduces the Coulombic repulsion between cations.

https://doi.org/10.1017/S0885715617001026 Published online by Cambridge University Press

TABLE III. Powder diffraction data for Pd_2HgSe_3 (Co$K\alpha$ radiation) (reflections with I_{obs} and $I_{calc} < 1$ are not shown in the table).

h	k	l	$2\theta_{obs}$ (°)	d_{obs} (Å)	I_{obs}	$2\theta_{calc}$ (°)	d_{calc} (Å)	I_{calc}	$2\theta_{obs} - 2\theta_{calc}$
1	0	0	16.244	6.3311	5	16.246	6.3304	5	−0.0018
0	0	1	19.495	5.2831	15	19.496	5.2829	15	−0.0006
0	1	1	25.480	4.0560	14	25.480	4.0561	14	0.0003
1	1	1	34.631	3.0052	10	34.626	3.0057	11	0.0049
2	0	1	38.469	2.7151	100	38.469	2.7152	100	0.0003
0	0	2	39.591	2.6411	1	39.586	2.6415	1	0.0050
0	1	2	43.054	2.4376	23	43.052	2.4378	13	0.0024
1	0	2				43.052	2.4378	10	
1	2	1	48.461	2.1794	5	48.459	2.1795	5	0.0022
0	2	2	52.343	2.0280	53	52.342	2.0280	44	0.0012
2	0	2				52.342	2.0280	7	
0	3	1	54.325	1.9593	3	54.317	1.9596	1	0.0079
3	0	1				54.317	1.9596	2	
2	2	0	58.613	1.8274	29	58.611	1.8274	29	0.0018
1	2	2	60.584	1.7733	11	60.583	1.7733	6	0.0009
2	1	2				60.583	1.7733	4	
2	2	1	62.392	1.7269	1	62.386	1.7270	1	0.0058
1	0	3	63.638	1.6965	8	63.636	1.6966	8	0.0022
3	1	1	64.942	1.6661	2	64.939	1.6661	2	0.0028
1	1	3	68.639	1.5865	7	68.641	1.5864	7	−0.0017
0	2	3	71.077	1.5389	7	71.078	1.5388	7	−0.0007
0	4	1	72.316	1.5160	15	72.315	1.5160	15	0.0014
1	3	2	75.434	1.4621	5	75.429	1.4622	2	0.0051
3	1	2				75.429	1.4622	3	
2	1	3	78.194	1.4183	6	78.200	1.4183	6	−0.0060
0	4	2	82.423	1.3576	10	82.427	1.3576	1	−0.0038
4	0	2				82.427	1.3576	9	
1	4	1	84.019	1.3365	2	84.022	1.3365	2	−0.0033
2	2	3	89.713	1.2681	11	89.722	1.2680	10	−0.0092
4	2	1	100.102	1.1668	13	100.100	1.1668	13	0.0020
2	4	2	110.327	1.0898	10	110.326	1.0898	1	0.0008
4	2	2				110.326	1.0898	9	
2	2	4	113.351	1.0705	5	113.358	1.0704	5	−0.0074

Hg atoms show three short Pd and Se contacts at 2.837(1) and 2.918(2) Å. For the sake of convenient structure description, Hg atoms can be considered to occupy the anti-cubooctahedral voids formed by Se atoms with the 3 + 6 + 3 bonding scheme. However, the next six and three Se atoms are at distances of 3.698(2) and 3.834(2) Å, respectively, and thus represent only weak Hg–Se bonds. In addition, Hg atom has three Pd contacts at 2.837(1) Å forming [$HgPd_3$] trigonal pyramid (Figure 3). Selected interatomic distances compared with those found in isostructural Pt_2HgSe_3 are summarized in Table IV. The relatively high values of displacement parameters (U_{iso}) of Pd(2), Hg, and Se atoms (see Table II) might be an indirect indication of possible structural disorder; however, no broad peaks or apparent peak asymmetry have been observed in powder diffraction pattern of Pd_2HgSe_3.

The crystal structure of Pd_2HgSe_3 can also be described as a $2a.2a.c$ superstructure of $PtSe_2$ structure, where Pt atoms and one-quarter of Se atoms have been replaced by Pd and Hg

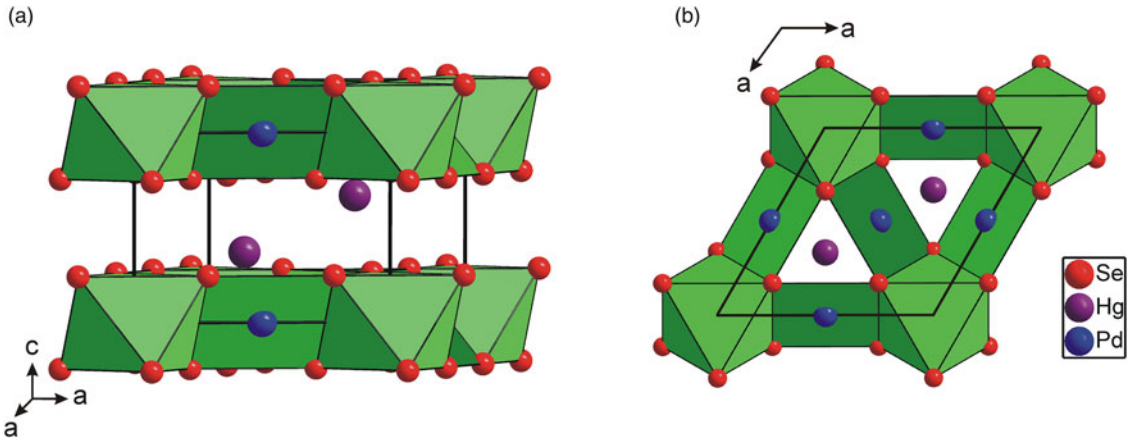

Figure 2. (Color online) Polyhedral representation of Pd_2HgSe_3 crystal structure showing the [Pd(1)Se_6] octahedra and [Pd(2)Se_4] squares. (a) Perspective view, (b) view along the c-axis.

https://doi.org/10.1017/S0885715617001026 Published online by Cambridge University Press

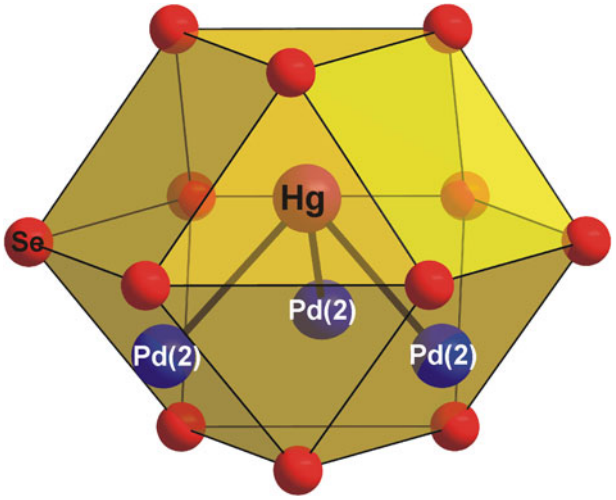

Figure 3. (Color online) The coordination polyhedra of Hg in the Pd_2HgSe_3 crystal structure.

TABLE IV. Selected interatomic distances (Å) in isostructural compounds Pd_2HgSe_3 and Pt_2HgSe_3.

Pd_2HgSe_3 (this work)			Pt_2HgSe_3 (Vymazalová *et al.*, 2012)		
Pd(1)	6 × Se	2.526(2)	Pt(1)	6 × Se	2.648(3)
Pd(2)	4 × Se	2.478(2)	Pt(2)	4 × Se	2.430(3)
	2 × Hg	2.837(1)		2 × Hg	2.819(2)
Hg	3 × Pd(2)	2.837(1)	Hg	3 × Pt(2)	2.819(2)

atoms, respectively. $PtSe_2$, which is also known as a mineral sudovikovite, adopts a layered structure of the CdI_2-structure type (Furuseth *et al.*, 1965). The corresponding group–subgroup relation is $P\bar{3}m1(k4/2a.2a.c)P\bar{3}m1$ and is shown in Figure 4. The splitting of Wyckoff position in the space group $P\bar{3}m1$ was constructed using the programme Wycksplit (Kroumova *et al.*, 1998).

Apart from its isostructural compounds (see above), the most closely structural related phase to Pd_2HgSe_3 is the mineral temagamite, Pd_3HgTe_3 (Laufek *et al.*, 2016). Both crystal structures show trigonal symmetry and Pd_3HgTe_3 shows

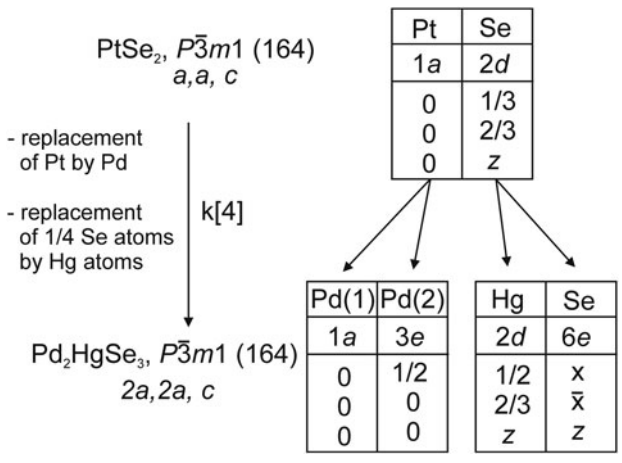

Figure 4. The group–subgroup relation between the $PtSe_2$ and Pd_2HgSe_3 structures including splitting of the Wyckoff positions.

approximately similar unit-cell parameter *a* [7.8211(6) Å]. The crystal structure of Pd_3HgTe_3 was described as being composed of layered modules (denoted as A through F) stacked along the *c*-axis. The modules B and F in temagamite structure show the same bond topology of Pd and Te atoms as Pd and Se atoms in Pd_2HgSe_3. Hg atoms occupy the anti-cubooctahedral voids in both compounds. The crystal structure of another Pd–Hg selenide, the mineral tischendorfite $Pd_8Hg_3Se_9$ (Laufek *et al.*, 2014), differs from Pd_2HgSe_3 to a certain extent. On one hand, Pd and Se atoms in $Pd_8Hg_3Se_9$ show different bond topology. On the other hand, Hg atoms have essentially identical coordination in both compounds. The crystal structure of a third known Pd–Hg selenide, the phase Pd_5HgSe (Laufek *et al.*, 2012), is based on $[HgPd_{12}]$ cubooctahedra and $[SePd_8]$ rectangular prism, and hence deviates significantly from the structure of Pd_3HgSe_2.

SUPPLEMENTARY MATERIAL

The supplementary material for this article can be found at https://doi.org/10.1017/S0885715617001026.

ACKNOWLEDGEMENTS

This work was supported by the internal projects Nos. 332000 and 331400 from the Czech Geological Survey. The authors thank Jan Drahokoupil (Institute of Physics of the Czech Academy of Sciences) for assistance in XRD data collection.

Bérar, J. F. and Baldinozzi, G. (**1993**). "Modeling of line-shape asymmetry in powder diffraction," J. Appl. Crystallogr. **26**, 128–129.

Bronger, W. and Bonsmann, B. (**1995**). "Ternare Thalliumplatin- und Thaliumpalladiumchalkogenide $Tl_2M_4S_6$. Synthesen, Kristallstruktur und Bindungsverhältnisse," Z. Anorg. Allg. Chem. **621**, 2083–2088.

Bruker AXS (**2014**) *Topas 5* (Karslruhe, Germany).

Drábek, M., Vymazalová, A., and Laufek, F. (**2014**). "The system Hg–Pd–Se at 400 °C: phase relations involving tischendorfite and other ternary phases," Can. Mineral. **52**, 763–768.

Earley, J. W. (**1950**). "Description and syntheses of the selenide minerals," Am. Mineral. **35**, 337–364.

Furuseth, S., Selte, K., and Kjekshus, A. (**1965**). "Redetermined crystal structures of $NiTe_2$, $PdTe_2$, PtS_2, $PtSe_2$," Acta Chem. Scand. **19**, 257–258.

Kroumova, E., Perez-Mato, J. M., and Aroyo, M. I. (**1998**). "WYCKSPLIT: a computer program for determination of the relations of Wyckoff positions for a group subgroup pair," J. Appl. Crystallogr. **31**, 646.

Laufek, F., Vymazalová, A., Drábek, M., and Drahokoupil, J. (**2011**). "Crystallographic study of Pd(Pt)-Hg-Se ternary systems," Mater. Struct. **18**(2), 124–125.

Laufek, F., Vymazalová, A., Drábek, M., Navrátil, J., Plecháček, T., and Drahokoupil, J. (**2012**). "Crystal structure and transport properties of Pd_5HgSe," Solid State Sci. **14**(10), 1476–1479.

Laufek, F., Vymazalová, A., Drábek, M., Navrátil, J., Drahokoupil, J. (**2014**). "Synthesis and crystal structure of tischendorfite $Pd_8Hg_3Se_9$," Eur. J. Mineral. **25**, 157–162.

Laufek, F., Vymazalová, A., Drábek, M., Dušek, M., Navrátil, J., Černošková, E. (**2016**). "The crystal structure of Pd_3HgTe_3, the synthetic analogue of temagamite," Eur. J. Mineral. **28**, 825–834.

Louër, D. and Boultif, A. (**2007**). "Powder pattern indexing and the dichotomy algorithm," Z. Kristallogr. **26**, 191–196.

Paar, W. H., Roberts, A. C., Criddle, A. J., and Topa, D. (**1998**). "A new mineral, chrisstanleyite, $Ag_2Pd_3Se_4$, from Hope's nose, Torquay, Devon, England," Mineral. Mag. **62**, 257–264.

Pauling, L. (**1929**). "The principles determining the structure of complex ionic crystal," J. Am. Chem. Soc. **51**, 1010–1026.

https://doi.org/10.1017/S0885715617001026 Published online by Cambridge University Press

Rodriguez-Carvajal, J. (**1990**). "FullProf: A program for Rietveld refinement and pattern matching analysis," in Satellite Meeting on Powder Diffraction of the XV Congress of the IUCr, Tolouse, France, p. 127.

Stanley, C. J., Criddle, A. J., Förster, H. J., and Roberts, A. C. (**2002**). "Tischendorfite, $Pd_8Hg_3Se_9$, a new mineral species from Tilkerode, Harz Mountains, Germany," Can. Mineral. **40**, 739–745.

Terada, K. and Cagle, F. W. Jr. (**1960**). "The crystal structure of potarite (Pd Hg) with some comments on allopalladium," Am. Mineral., **45**, 1093–1097.

Vymazalová, A., Laufek, F., Drábek, M., Cabral, A. R., Haloda, J., Sidorinová, T., Lehmnn, B., Galbiatti, H. F., and Drahokoupil, J. (**2012**). "Jacutingaite, Pt_2HgSe_3, a new platinum-group mineral from the Cauê iron-ore deposit, Itabira District, Minas Gerais, Brazil," Can. Mineral. **50**(2), 431–440.

https://doi.org/10.1017/S0885715617001026 Published online by Cambridge University Press